Cross laminated timber at in-plane beam loading – New analytical model predictions and relation to EC5

Jeleč, Mario; Danielsson, Henrik; Serrano, Erik; Rajčić, Vlatka

Published in:
International Network on Timber Engineering Research

2018

Document Version:
Publisher's PDF, also known as Version of record

Cross laminated timber at in-plane beam loading – New analytical model predictions and relation to EC5

Mario Jeleč, Department of Materials and Structures, University of Osijek, Croatia

Henrik Danielsson, Division of Structural Mechanics, Lund University, Sweden

Erik Serrano, Division of Structural Mechanics, Lund University, Sweden

Vlatka Rajčić, Department of Structures, University of Zagreb, Croatia

Keywords: CLT, beam, in-plane loading, shear failure, lay-up, FE-analysis

1 Introduction

Beams made of cross laminated timber (CLT) offer several advantages over solid or glued laminated timber beams. Thanks to their orthogonal laminar structure, the transversal layers have a reinforcing effect with respect to the stress perpendicular to the beam axis. Due to the layered composition of CLT, the stress state is however complex and several failure modes and geometry parameters need to be considered in design. Several experimental tests on CLT beams have been conducted, e.g. by Bejtka (2011), Flaig (2013) and Danielsson *et al* (2017a, 2017b).

An analytical model for stress analysis and strength verification has been presented by Flaig & Blass (2013), including stress based failure criteria for relevant failure modes. This model has been used as a basis for the design equations for CLT beams in the current draft version of the new Eurocode 5 (CEN/TC 250/SC5, 2018).

The model by Flaig & Blass includes two basic assumptions related to the shear stresses acting in the crossing areas between the longitudinal and transversal laminations and relevant for shear failure mode III: 1) the stresses are, irrespective of the element lay-up, uniformly distributed in the beam width direction and 2) the torsional moments/stresses are uniformly distributed over all crossing areas in the beam height direction. Based on comparison to 3D FE-analyses as presented by Jelec *et al* (2016) and Danielsson *et al* (2017a), both these assumptions seem to be inaccurate.

The aim of the paper is to present a new model in terms of improvements of the original analytical model by Flaig & Blass (2013). Model improvements as presented by Danielsson & Serrano (2018) are reviewed and further improvements of that model are also presented. The differences between the models concern internal force and stress distributions relevant for shear failure mode III of CLT beams. Predictions of the original and the new analytical models are compared to results of 3D FE-analyses and design proposals based on the new analytical model are presented.

2 Analytical model and relation to EC 5

A brief review of the model presented by Flaig & Blass (2013) for stress analysis and strength verification of shear failure mode III for CLT beams is presented below. The equations presented are based on notation according to Fig. 1 and relate to prismatic CLT beams without edge-bonding and composed of longitudinal laminations of width b_0 and transversal laminations of width b_{90}. The laminations are assumed to have identical stiffness properties.

Index *i* refers to the position of the longitudinal laminations in the beam height direction and index *k* refers to their position in the beam width direction. Cross sectional forces and moments are considered at four separate levels: (V, N, M) refer to the total forces and moment acting on the gross cross section, (V_k, N_k, M_k) refer to the total forces and moments acting in the *k*:th longitudinal layer consisting of *m* longitudinal laminations, (V_i, N_i, M_i) refer to the total forces and moments acting in the *k* longitudinal layers at position *i* in the beam height direction and ($V_{i,k}$, $N_{i,k}$, $M_{i,k}$) refer to the forces and the moment acting in an individual longitudinal lamination *i*,*k*.

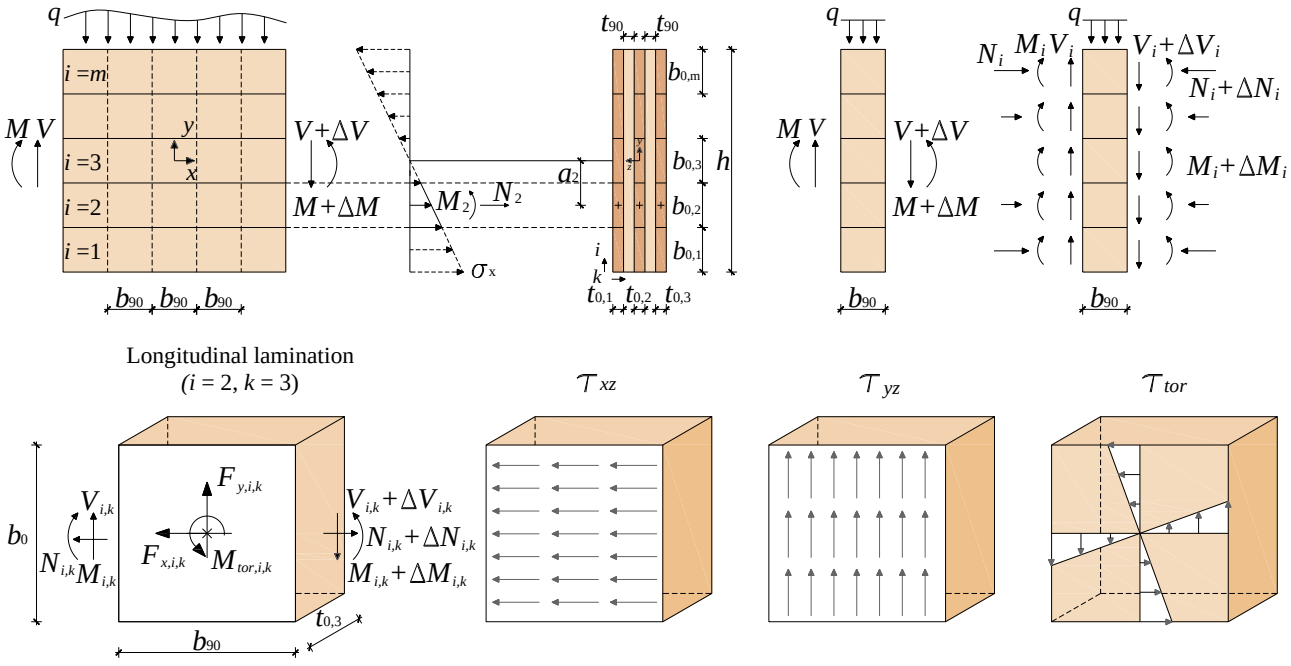

Figure 1. Illustration of beam model and definition of load and geometry parameters.

2.1 Shear mode III

According to the model presented by Flaig & Blass (2013), three shear stress components acting in the crossing area should be considered: (a) shear stress parallel to the beam axis τ_{xz}, (b) shear stress perpendicular to the beam axis τ_{yz} and (c) torsional shear stress τ_{tor}. Assumed shear stress distributions for a single crossing area are shown in Fig. 1. The *maximum* stresses for a beam composed of m longitudinal laminations in the beam height direction and having n_{CA} number of crossing areas in the beam width direction can, according to Flaig & Blass, be expressed as

$$\tau_{xz} = \frac{6V}{b_0^2}\frac{1}{n_{CA}}\left(\frac{1}{m^2} - \frac{1}{m^3}\right) \tag{1}$$

$$\tau_{yz} = \frac{q}{h}\frac{1}{n_{CA}} \tag{2}$$

$$\tau_{tor} = \frac{3V}{b_0^2}\frac{1}{n_{CA}}\left(\frac{1}{m} - \frac{1}{m^3}\right)k_b \quad \text{with } k_b = \frac{2b_{max}b_0}{b_0^2 + b_{90}^2} \tag{3}$$

where b_0 and b_{90} are the longitudinal and transversal lamination widths, respectively, and where $b_{max} = \max(b_0, b_{90})$.

For failure in the crossing areas, based on experimental tests of crossing areas loaded in either uni-axial shear, pure torsion, or a combination of both, failure criteria according to the following equations are proposed by Flaig & Blass (2013)

$$\frac{\tau_{tor}}{f_{v,tor}} + \frac{\tau_{xz}}{f_R} \leq 1.0 \tag{4}$$

$$\frac{\tau_{tor}}{f_{v,tor}} + \frac{\tau_{yz}}{f_R} \leq 1.0 \tag{5}$$

Test results indicate a mean value of the torsional strength of about $f_{v,tor} = 3.5$ MPa and a mean value of the rolling shear strength of about $f_R = 1.5$ MPa, according to Flaig & Blass (2013). The proposed failure criterion according to Eq. (5) includes shear stress perpendicular to the beam axis τ_{yz} which has local influence at supports and load introduction points. This shear stress component is not further considered here.

The shear stress parallel to the beam axis, τ_{xz}, increases with the distance from the neutral axis and Eq. (1) gives the *maximum* value which is found at the lower- and uppermost crossing areas in the beam height direction. The torsional moments and the torsional shear stress τ_{tor} are by assumption equal for all crossing areas in the beam height direction. Therefore, according to the stress interaction criterion given by Eq. (4), the upper- and lowermost crossing areas are the ones relevant for strength verification. Assuming equal torsional moments in the beam height direction corresponds from a static equilibrium point of view to assuming equal lamination shear forces in the beam height direction, i.e. $V_i = V/m$.

3 Model improvements – New analytical model

Improvements of the original model presented by Flaig & Blass (2013), concerning the distributions of internal forces and moments, are presented by Danielsson & Serrano (2018) and reviewed below.

3.1 Longitudinal lamination shear forces $V_{i,k}$

The shear force, *V*, is carried by the *longitudinal* laminations *only* at locations (in the beam length direction) corresponding to a section between adjacent transversal laminations without edge bonding. The shear force *V* is for these locations assumed to be distributed between the individual longitudinal laminations *i*,*k* according

$$V_{i,k} = \alpha_i \beta_k V \tag{6}$$

where α_i and β_k are dimensionless weighting factors defining the distribution in the beam height (α_i) and in the beam width (β_k) directions. The weighting factors α_i can be derived by considering the parabolic shear stress distribution τ_{xy} known from conventional engineering beam theory and shown in Fig. 2. Based on a dimensionless parabolic function *T*(*y*), the weighting factors α_i are expressed as

$$\alpha_i = \int_{-\frac{m}{2}+(i-1)}^{\frac{m}{2}+i} T(y)dy = \frac{6i - 6i^2 + m(6i-3) - 2}{m^3} \tag{7}$$

A distribution of the lamination shear forces in the beam width direction according to

$$\beta_k = \frac{t_{0,k}}{t_{net,0}} \tag{8}$$

with $t_{net,0} = \Sigma t_{0,k}$ is further assumed in the proposal by Danielsson & Serrano (2018).

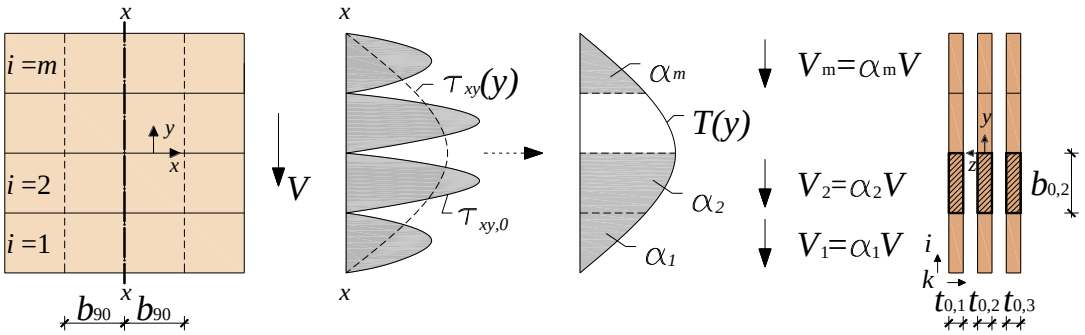

Figure 2. Illustration of shear force/stress distribution according to Danielsson & Serrano (2018).

3.2 Parallel to beam axis forces $F_{x,i,k}$ and stresses $\tau_{xz,i,k}$

The parallel to beam axis force $F_{x,i,k}$ balances the change in the lamination normal force $\Delta N_{i,k}$ over the length b_{90}, see Fig. 1. Considering constant normal stress in the beam width direction and a linear variation in the beam height direction, the parallel to beam axis forces $F_{x,i,k}$ can, by equilibrium considerations, be found as

$$F_{x,i,k} = \frac{12 V b_{90}}{m^3 b_0^2} \frac{1}{n_{CA,k}} \frac{t_{0,k}}{t_{net,0}} a_i \quad \text{with} \quad a_i = b_0 \left(\frac{m+1}{2} - i \right) \tag{9}$$

where a_i is the distance in the *y*-direction between the centre-line of the beam and the centre-line of lamination *i*,*k*. Assuming a uniform shear stress distribution over each crossing area gives

$$\tau_{xz,i,k} = \frac{12V}{m^3 b_0^3} \frac{1}{n_{CA,k}} \frac{t_{0,k}}{t_{net,0}} a_i \qquad (10)$$

The maximum parallel to beam axis shear stress with respect to the beam height direction is found at the lower- and uppermost crossing area. The stress distribution in the beam width direction is governed by the ratios of $t_{0,k}$, the longitudinal layer widths, to $n_{CA,k}$, the number of crossing areas that an individual longitudinal lamination shares with adjacent transversal laminations (= 1 or 2), i.e. $t_{0,k}/n_{CA,k}$.

3.3 Torsional moments $M_{tor,i,k}$ and stresses $\tau_{tor,i,k}$

Expressions for the torsional moments $M_{tor,i,k}$ and the torsional stresses $\tau_{tor,i,k}$ can be derived by considering equilibrium of a part of a single longitudinal lamination, see Fig. 1. For zero external load *q* and by using lamination shear forces $V_{i,k}$ according to Eq. (6), the torsional moments may be found as

$$M_{tor,i,k} = \frac{V b_{90}}{n_{CA,k}} \left(\alpha_i \beta_k - \frac{t_{0,k}}{t_{net,0}} \frac{1}{m^3} \right) \qquad (11)$$

with α_i and β_k as defined in Section 3.1. Assuming a torsional shear stress distribution according to Fig. 1, the *maximum* torsional shear stress, found at the mid-points of the four sides of crossing area *i*,*k,* is then given by

$$\tau_{tor,i,k} = \frac{3V}{b_0^2} \frac{1}{n_{CA,k}} \left(\alpha_i \beta_k - \frac{t_{0,k}}{t_{net,0}} \frac{1}{m^3} \right) k_b \quad \text{with } k_b = \frac{2 b_{max} b_0}{b_0^2 + b_{90}^2} \qquad (12)$$

Eqs. (11) and (12) give maximum values of the torsional moments and the torsional shear stresses at the crossing areas located closest to the beam centre-line, in-line with the lamination shear force distribution as discussed in Section 3.1.

4 Comparison between analytical and FE-models

Numerical parameter studies were carried out on 3D FE-models in order to investigate the distribution of internal forces and stresses in the beam height and the beam width directions, respectively. The FE-analyses were performed using Ansys 2018 and they present an extension of the FE-analyses presented by Danielsson *et al* (2017). Thus, the same considerations with respect to material (see Table 1) and contact properties, as well as loading and supporting conditions, were used.

Table 1. Material stiffness parameters used for FE-analyses

E_L [MPa]	E_T [MPa]	E_R [MPa]	G_{LT} [MPa]	G_{LR} [MPa]	G_{TR} [MPa]	ν_{LT} [-]	ν_{LR} [-]	ν_{RT} [-]
12000	400	600	750	600	75	0.50	0.50	0.33

The analyses of force and moment distributions in the beam height and width directions were carried out separately considering 3-layer elements (3s) and 5-layer elements (5s), respectively. Due to the highly non-uniform shear stress distributions within the individual crossing areas, results are presented in the form of resulting forces and moments obtained from FE-models by integration of stresses over relevant areas. An illustration of the considered beam geometry and notation for considered forces and moments is shown in Fig. 3. Several influencing parameters were investigated with the underlined values used as reference values:

- Number of laminations in the beam height direction (m = 2 … **4** … 8)
- Lamination width ($b = b_0 = b_{90}$ = 100, **150**, 200 mm)
- Width of gap between laminations (t_{gap} = **0.1**, 1, 5 mm)
- Element lay-up for 5-layer elements ($t_{0,2}/t_{0,1} = t_{0,2}/t_{0,3}$ = 0.31 … **2.0** … 2.62)
- Transversal layer width (t_{90} = 10, **20**, 30 mm)
- Contact stiffness (K = 10, **100**, 1000 N/mm^3)
- Approximate FE-mesh size (4, 5, **10** mm)

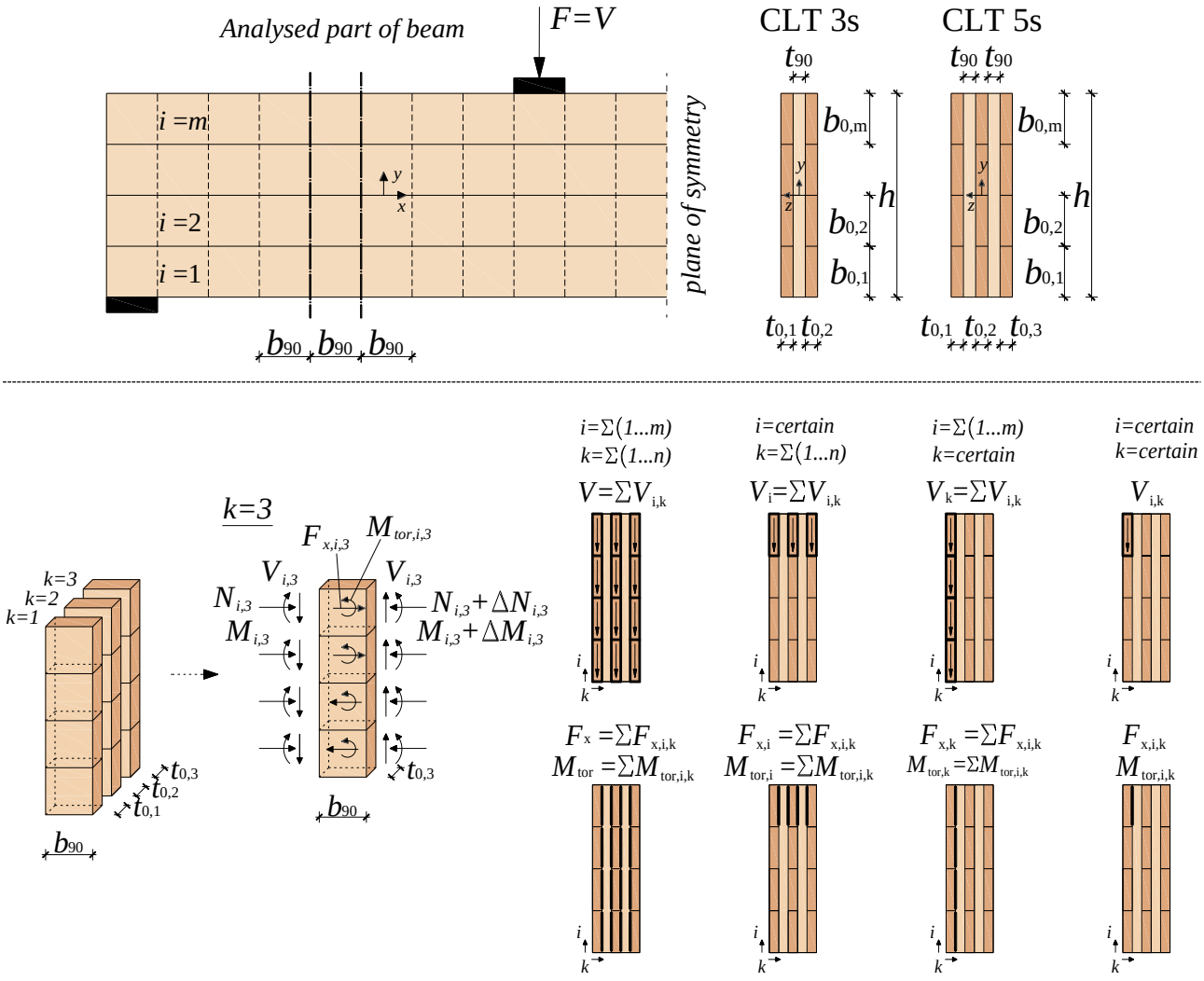

Figure 3. Illustration of geometry and considered forces of FE-analysis

The FE-results presented below are based on reference values of parameters as stated above according to: $b_0 = b_{90} = 150$ mm, $t_{gap} = 0.1$ mm, $K = 100$ N/mm^3 and a FE-mesh based on cubically shaped elements with a side length of about 10 mm. FE-analyses considering other values of parameters as stated above were also carried out but were found to yield only very small influence on the results.

4.1 Results regarding force distribution in the beam height direction

A parameter study of the force distribution in the beam height direction was carried out on 3-layer elements with lay-up 40-20-40, by varying the number of longitudinal laminations m from 2 to 8. Results according to the FE-analyses, the analytical model presented by Flaig & Blass (2013) and the proposed new model are presented for the shear forces V_i in Fig. 4, for the torsional moments $M_{tor,i}$ in Fig. 5 and for the parallel to beam axis forces $F_{x,i}$ in Fig. 6. Forces and moments are presented in a normalized manner as V_i/V, $M_{tor,i}/M_{tor}$ and $F_{x,i}/F_x$ with definitions according to Fig. 3.

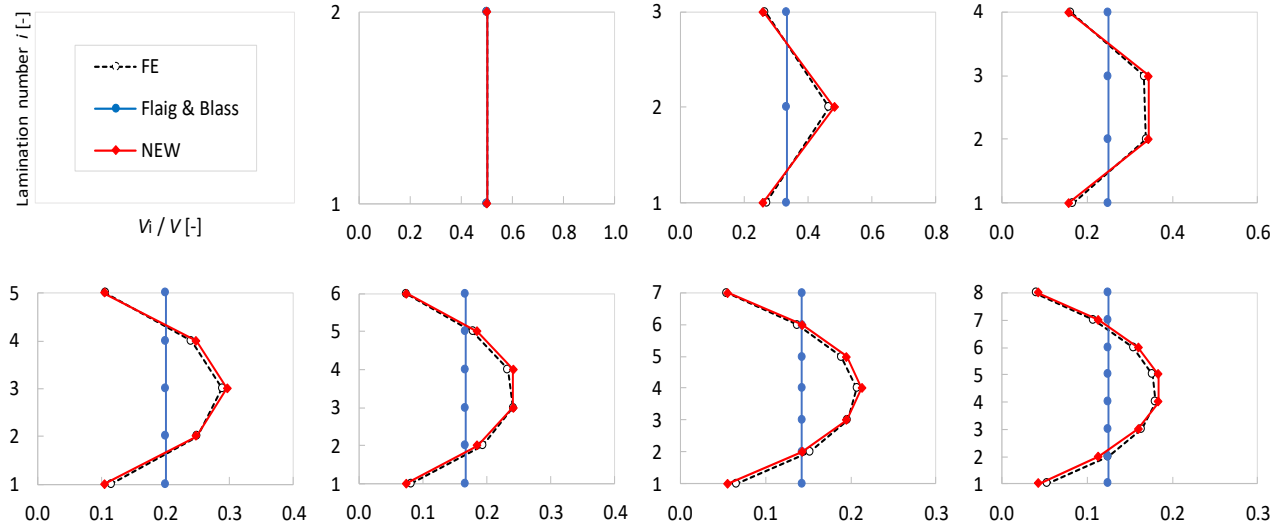

Figure 4. Distribution of shear forces in the beam height direction for CLT 3s (40-20-40).

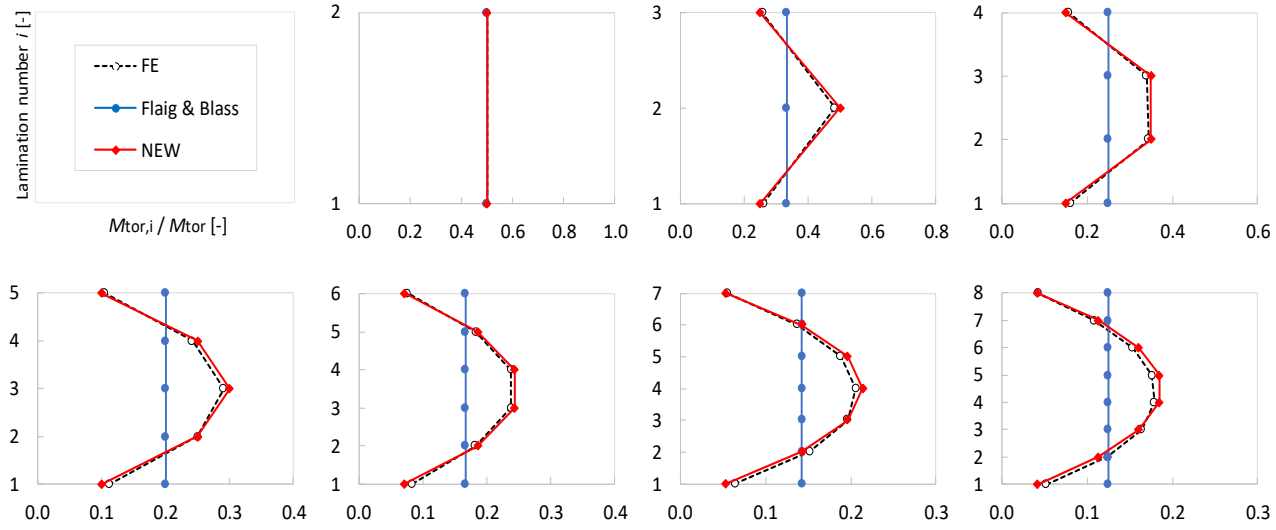

Figure 5. Distribution of torsional moments in the beam height direction for CLT 3s (40-20-40).

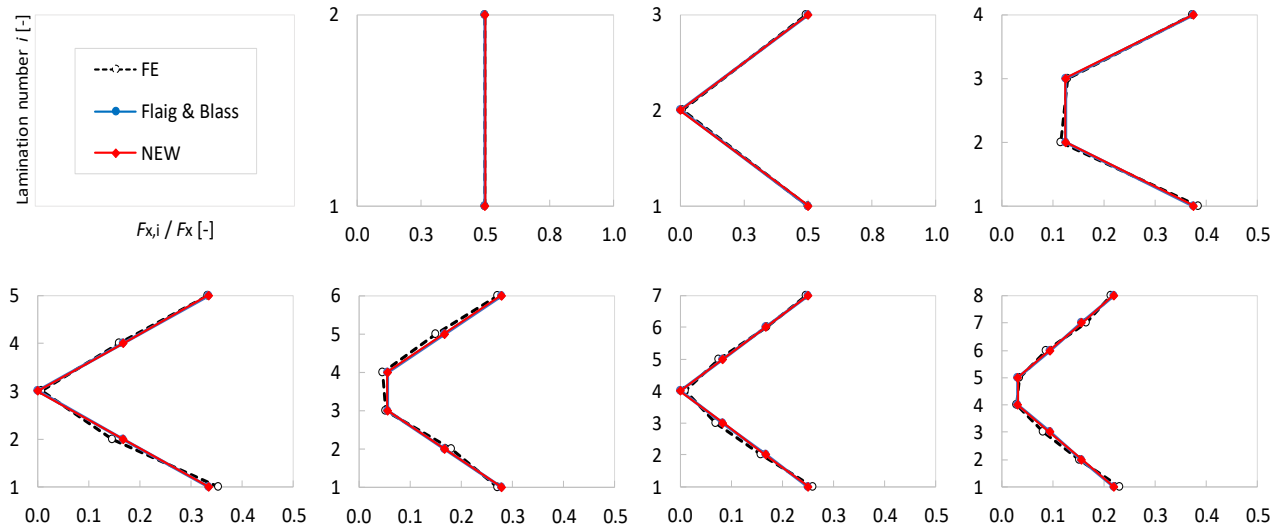

Figure 6. Distribution of parallel to beam axis forces in the beam height direction, CLT 3s (40-20-40).

The graphs presented in Figs. 4 and 5 show very good agreement between FE-results and the new analytical model. Both the FE-analyses and the new analytical model predict significantly higher values of the shear forces V_i and the torsional moments $M_{tor,i}$ close to the beam centre-line than in the upper and lower parts of the beam. The analytical model presented by Flaig & Blass assumes constant torsional moments in the beam height direction, which also corresponds to constant laminations shear forces in that direction. Hence, that model underestimates the torsional moments close to the beam centre-line and overestimates the torsional moments in the upper and lower parts of the beam. The respective ratios V_i/V and $M_{tor,i}/M_{tor}$ according to the new analytical model are very similar, but not identical.

The comparison of the absolute values of the parallel to beam axis forces $F_{x,i}$, as presented in Fig. 6, show very good agreement between results of the FE-analyses and both analytical models. The two analytical models predict the same forces $F_{x,i,k}$ and shear stresses $\tau_{xz,i,k}$ since the ratio $t_{0,k}/n_{CA,k}$ is constant for 3-layer elements and the assumption of equal shear stress distribution in the beam width direction hence is valid.

4.2 Results regarding force distribution in the beam width direction

A parameter study of the force distribution in the beam width direction was carried out on 5-layer elements composed of $m = 4$ longitudinal laminations in the beam height direction. The influence of the element lay-up was investigated by considering ratios of interior to exterior longitudinal layer widths in the range $t_{0,2}/t_{0,1} = t_{0,2}/t_{0,3} = 0.31 \ldots 2.62$ for a fixed net cross section width $t_{net,0} = t_{0,1} + t_{0,2} + t_{0,3} = 120$ mm.

Results for shear forces V_k, torsional moments $M_{tor,k}$ and parallel to beam axis force $F_{x,k}$ are presented in Fig. 7 using definitions according to Fig. 3. Results for shear forces V_k are presented as normalized with respect to the total shear force V (upper left) and also as normalized with respect to the total shear force V and the relative longitudinal layer width $t_{0,k}/t_{net,0}$ (lower left). Results for $M_{tor,k}$ and $F_{x,k}$ are presented in a similar manner: normalized with respect to the totals M_{tor} and F_x (upper centre and upper

right) and also normalized by the totals M_{tor} and F_x, the relative longitudinal layer width $t_{0,k}/t_{net,0}$ and the number of crossing areas $n_{CA,k}$ (lower centre and lower right). For the lower row of Fig. 7, the value 1.0 represents forces and torsional moments as predicted by the new analytical model presented in Section 3.

FE-results regarding the parallel to beam axis forces $F_{x,k}$ and their distribution in the beam width direction agree very well with predictions according to the new analytical model as presented in Section 3. The shear forces and torsional moments found from the FE-analyses show, however, partly different distributions in the beam width direction compared to the new analytical model. For the lay-up $t_{0,2}/t_{0,1} = t_{0,3}/t_{0,1} = 2.0$, the distribution of lamination shear forces V_{ik} according to Eq. (6) using $\beta_k = t_{0,k}/t_{net,0}$ according to Eq. (8) agrees very well with the FE-results. For $t_{0,2}/t_{0,1} = t_{0,3}/t_{0,1} \leq 2.0$, the FE-analyses yield larger shear forces and torsional moments for the interior longitudinal layer ($k = 2$) compared to the analytical model predictions.

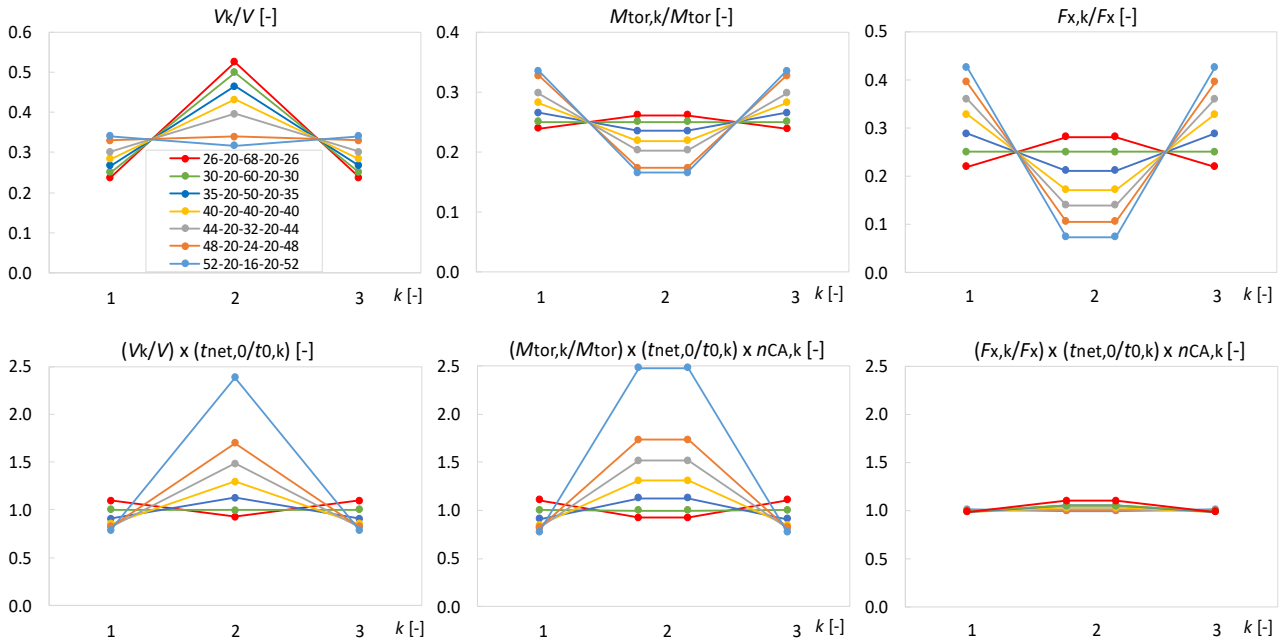

Figure 7. FE-results of influence of lay-up on distribution in beam width direction for CLT element 5s.

Alternative expressions for the weighting factors β_k were determined by manual curve-fitting to the shear force distribution found from the FE-analyses. Weighting factors according to

$$\beta_k = \begin{cases} \frac{1}{8}\left(1 + 4\frac{t_{0,k}}{t_{net,0}}\right) & \text{for } k = 1,3 \\ \frac{1}{4}\left(1 + 2\frac{t_{0,k}}{t_{net,0}}\right) & \text{for } k = 2 \end{cases} \tag{13}$$

where found to yield good agreement for the 5-layer element lay-ups considered in the parameter study. For the special case of $t_{0,2}/t_{0,1} = t_{0,2}/t_{0,3} = 2.0$ with constant ratio $t_{0,k}/n_{CA,k}$, Eq. (13) gives the same weighting factors β_k as Eq. (8). Weighting factors β_k

given in Eq. (13) are not included in the model by Danielsson & Serrano (2018) and hence represent an extension of that model.

A comparison between FE-results and the new analytical model is presented in Fig. 8 regarding lamination shear forces V_k, torsional moments $M_{tor,k}$ and parallel to beam axis forces $F_{x,k}$. The marks represent FE-results and predictions according to the new analytical model as presented in Section 3 are represented by solid lines. Dashed lines represent the shear forces V_k and the torsional moments $M_{tor,k}$ according to the new analytical model and use of weighting factors β_k according to Eq. (13).

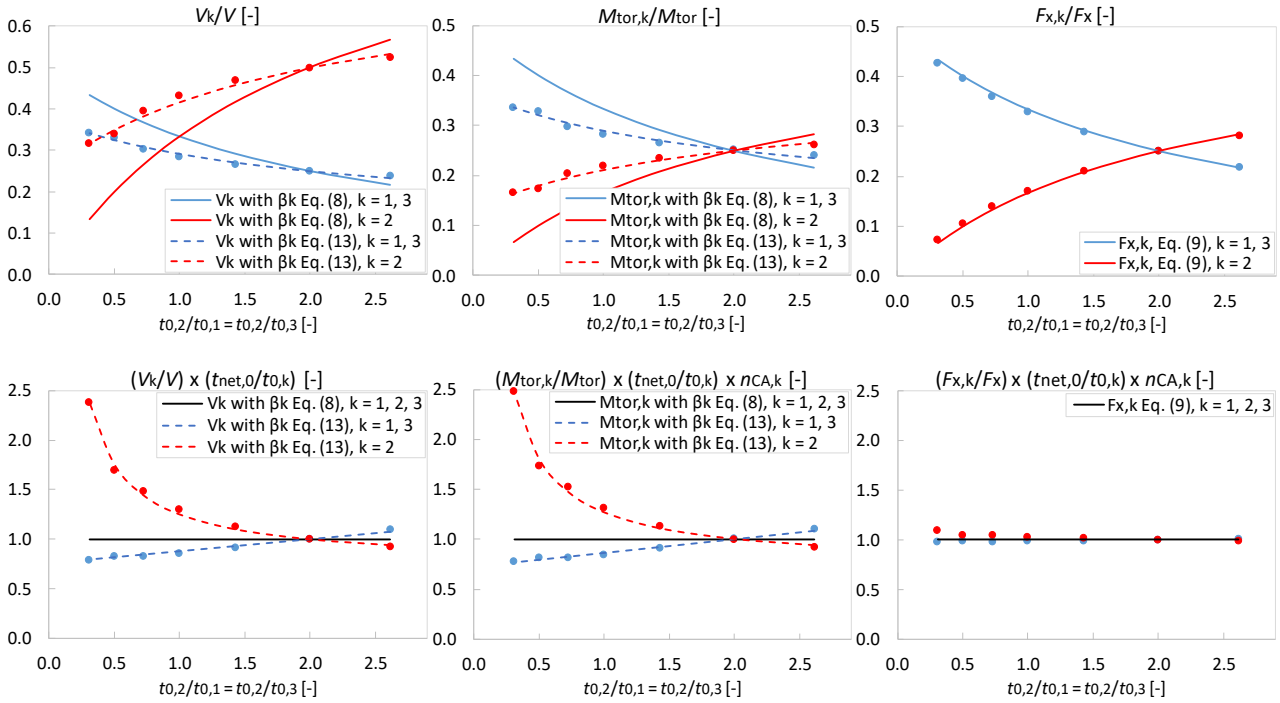

Figure 8. Comparison between FE-results (marks) and proposed new model (lines) regarding the influence of the element lay-up on the distribution of forces in the beam width direction for CLT 5s.

5 Discussion and background of design proposals

The original model according to Flaig & Blass (2013) and new model improvements have here been compared to a numerical model based on 3D FE-analyses. The non-uniform distribution of the torsional moments $M_{tor,i,k}$ in the beam height direction based on weighting factors α_i as proposed by Danielsson & Serrano (2018) shows very good agreement with the FE-results. It is further evident that the element lay-up in terms of the relative longitudinal layer widths $t_{0,k}/t_{net,0}$ and the ratio $t_{0,k}/n_{CA,k}$ influence the stress distribution in the beam width direction.

The distributions of the lamination shear forces $V_{i,k}$ and the torsional moments $M_{tor,i,k}$ in the beam width direction based on β_k according to Eq. (8) differ partly compared the FE-results. For 5-layer CLT elements typically used in practice, with lay-ups in the range of $0.5 \leq t_{0,2}/t_{0,1} = t_{0,2}/t_{0,3} \leq 1.0$, the maximum torsional moment is found for crossing areas at the exterior longitudinal layers, i.e. for $k = 1, 3$. Within this range of lay-ups

and for the exterior crossing areas, the torsional moments $M_{tor,i,k}$ according to Eq. (11) with β_k according to Eq. (8) are about 20% higher than found from the FE-analyses. Regarding practical design, calculation of the torsional moments in this manner hence yields a (safe side) overestimation compared to the FE-results. The alternative expression for β_k according to Eq. (13) gives good agreement with the FE-results.

The maximum torsional moment and the maximum parallel to beam axis force occur at different crossing areas, see Figs. 5 and 6. Using the failure criterion in Eq. (4) with the maximum value of $\tau_{xz,i,k}$ according to Eq. (10) and the maximum value of $\tau_{tor,i,k}$ according to Eq. (12) would then be mechanically incorrect (and conservative).

Since the failure criterion in Eq. (4) is based on consideration of two different shear strengths, $f_{v,tor}$ and f_R, it is not straightforward to determine which crossing area that is mostly stressed. Distributions of the maximum values of $\tau_{tor}/f_{v,tor}$, τ_{xz}/f_R and $\tau_{tor}/f_{v,tor} + \tau_{xz}/f_R$ for the individual crossing areas in the beam height direction are presented in Fig. 9, considering a fixed ratio of the strength values as $f_{v,tor}/f_R = 3.5/1.5 = 2.33$. The stress components are normalized in such a way that $\max\{\tau_{tor}/f_{v,tor} + \tau_{xz}/f_R\} = 1.0$. The critical crossing areas are here found as either the two most centrically placed (m = even) or the two crossing areas placed next to the centric crossing area (m = odd).

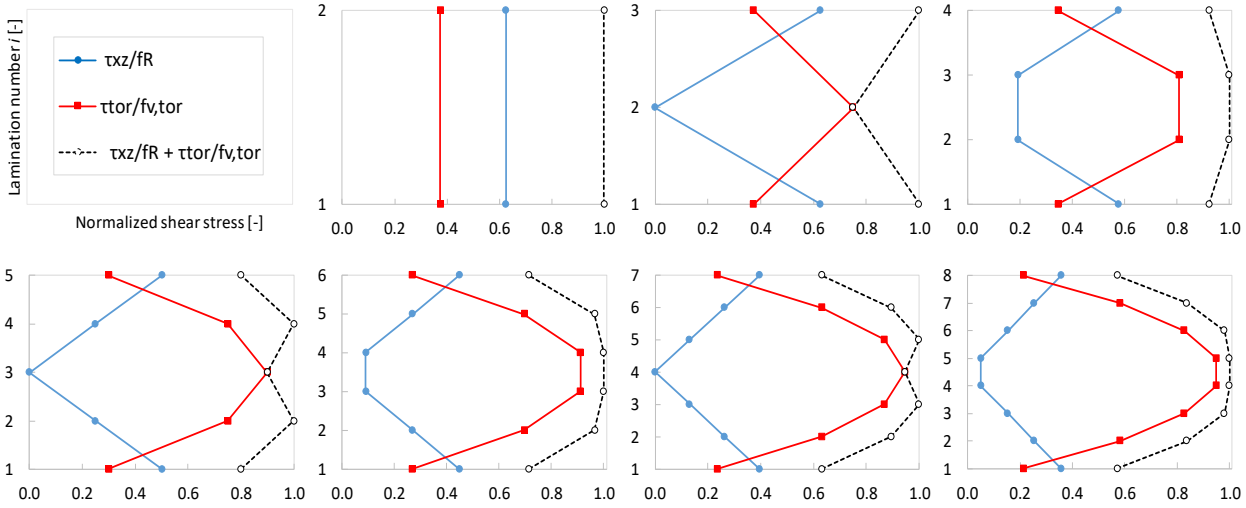

Figure 9. Distributions of $\tau_{tor}/f_{v,tor}$, τ_{xz}/f_R and $\tau_{tor}/f_{v,tor} + \tau_{xz}/f_R$ in beam height direction for $2 \le m \le 8$ for CLT beam 5s (40-20-40-20-40) considering β_k according to Eq. (13) and $b_0 = b_{90} = 150$ mm

For practical design purposes, it is desirable to increase the ease-of-use by finding reasonably simple expressions for the torsional shear stress τ_{tor} and the parallel to beam axis shear stress τ_{xz} for the critical crossing area, irrespective of m being odd or even. Two designs proposals are presented in Section 6, based on the discussion and comparisons presented in Sections 5.1 and 5.2.

5.1 Background of design proposal 1

An approximation of τ_{xz} for the critical crossing area can be found from Eq. (10) by considering $a_i = b_0/2$, giving

$$\tau_{xz} = \frac{6V}{b_0^2} \frac{1}{n_{CA,k}} \frac{t_{0,k}}{t_{net,0}} \frac{1}{m^3} \qquad (14)$$

which is exact for even numbers *m* compared to the analytical model as presented in Section 3 and shown in Fig. 9. For odd *m*, Eq. (14) represents an overestimation of τ_{xz} for the centrically placed crossing area and an underestimation of τ_{xz} for the critical crossing areas placed next to the centric one.

The maximum torsional shear stress according to Eq. (12) is determined by the maximum value of α_i according to Eq. (7). Considering the two cases of even and odd number of longitudinal laminations in the beam height direction separately, exact maximum values of α_i are given by

$$\max\{\alpha_i\} = \frac{3m^2 - 4}{2m^3} \qquad \text{for } m = 2, 4, 6 \ldots \qquad (15)$$

$$\max\{\alpha_i\} = \frac{3m^2 - 1}{2m^3} \qquad \text{for } m = 3, 5, 7 \ldots \qquad (16)$$

The maximum values of α_i for the general case given by Eq. (7) and according to Eqs. (15) and (16) are illustrated in Fig. 10. Eq. (15) yields an underestimation of the maximum value of τ_{tor} for odd *m* while Eq. (16) yields an overestimation of the maximum value of τ_{tor} for even *m*. For the critical crossing areas, Eq. (15) does however yield an overestimation of the design relevant value of τ_{tor} also for odd *m* since the critical crossing area is placed next to the most centric crossing area.

To arrive at reasonably simple expressions for design purposes, the torsional shear stress in the critical crossing area can be determined using Eq. (12) with $\max\{\alpha_i\}$ according to Eq. (15) while the parallel to beam axis shear in the critical crossing area can be determined using Eq. (14). This approach yields exact results compared to the analytical model as presented in Section 3 for even *m*. For odd *m*, the underestimation of τ_{xz} in the critical crossing area is compensated by an overestimation of τ_{tor} in the same crossing area and overall accurate predictions are obtained. This proposal is presented in Section 6 as design proposal 1.

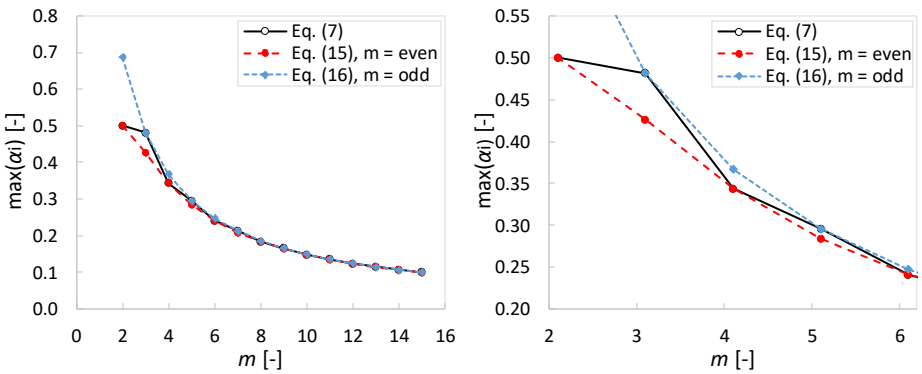

Figure 10. Comparison of max{α_i} according to Eqs. (7), (15) and (16) for 2 ≤ m ≤ 15.

5.2 Background of design proposal 2

To arrive at more simplified design equations compare to proposal 1, the factors α_i and β_k can be combined into a single factor γ. The maximum torsional shear stress according to Eq (12) may then be expressed as

$$\tau_{tor} = \frac{3V}{b_0^2}\frac{t_{0,k}}{t_{net,0}}\left(\frac{1}{m}-\frac{1}{m^3}\right)k_b\gamma \qquad (17)$$

where the dimensionless factor γ is given by

$$\gamma = \frac{\left[max\{\alpha_i\}\beta_1\left({}^{t_{net,0}}/_{t_{0,k}}\right)-{}^{1}/_{m^3}\right]}{\left({}^{1}/_{m}-{}^{1}/_{m^3}\right)} \qquad (18)$$

Exact values of the factors γ according to Eq. (18) are shown in Fig. 11 for CLT 5s with $2 \le m \le 15$ and for the two options of β_1; as defined in Section 3 and denoted as γ_1 and as found by curve-fitting to FE-results in Section 4 and denoted as γ_2, respectively. Weighting factors α_i are according to Eq. (7). Based on this, simplifications as illustrated in Fig. 11 (right) can be made to avoid including the factors α_i and β_k in the design equations. A conservative simplification is $\gamma_1 = 1.5$, based on the maximum value of γ using β_1 according to Eq. (8). Another simplification, and in relation to the presented FE-results an overall more accurate one, can be made based on the mean values of the factors γ, denoted as γ_2, within the interval $3 \le m \le 15$ for each of the individual lay-ups and using β_1 according to Eq. (13). The conservative simplification $\gamma_1 = 1.5$ is valid also for CLT 3s.

Concerning τ_{xz}, approximation according to Eq. (14) may be used also here. This proposal is presented in Section 6 as design proposal 2.

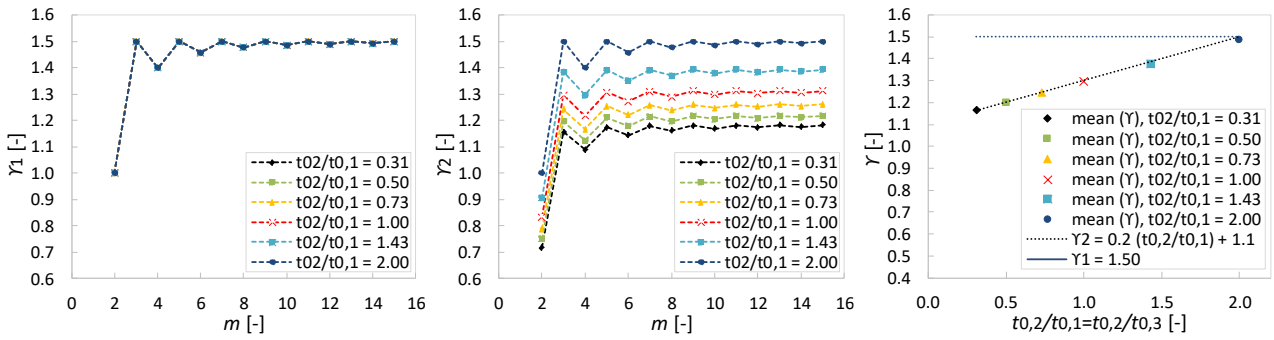

Figure 11. Factors γ_1 and γ_2 according to Eq. (18) with β_k according to Eq. (8) (left) and Eq. (13) (centre) and the mean values of γ_1 and γ_2 within the interval $3 \le m \le 15$ for different lay-ups of CLT 5s (right).

6 Design proposals and concluding remarks

Two alternative design proposals are presented below, based on the discussion in the previous section. Both proposals are based on:

- comparison of forces and moments between analytical and FE-analyses,

- crossing area shear stress distributions as illustrated in Fig. 1,
- shear mode III failure criterion according to Eq. (4) with a ratio between the proposed strength values as $f_{v,tor}/f_R \approx 2.3$.

Design proposal 1 is aimed at being as exact as possible in relation to the FE-results while keeping design equations fairly simple. Design proposal 2 is aimed at obtaining further simplification of the design equations while yet retaining as much as possible of the important design aspects and being exact or conservative in relation to the FE-results.

6.1 Design proposal 1

Design relevant crossing area shear stresses τ_{xz} and τ_{tor} are approximated as

$$\tau_{xz} = \frac{6V}{b_0^2}\frac{t_{0,1}}{t_{net,0}}\frac{1}{m^3} \tag{19}$$

$$\tau_{tor} = \frac{3V}{b_0^2}\left(\alpha_{i,max}\beta_1 - \frac{t_{0,1}}{t_{net,0}}\frac{1}{m^3}\right)k_b \qquad \text{with } k_b = \frac{2b_{max}b_0}{b_0^2 + b_{90}^2} \tag{20}$$

where

$$\alpha_{i,max} = \frac{3m^2 - 4}{2m^3} \tag{21}$$

$$\beta_1 = \begin{cases} \dfrac{t_{0,1}}{t_{net,0}} & \text{for 3-layer CLT beams} \\ \dfrac{1}{8}\left(1 + 4\dfrac{t_{0,1}}{t_{net,0}}\right) & \text{for 5-layer CLT beams} \end{cases} \tag{22}$$

6.2 Design proposal 2

Design relevant crossing area shear stresses τ_{xz} and τ_{tor} are approximated as

$$\tau_{xz} = \frac{6V}{b_0^2}\frac{t_{0,1}}{t_{net,0}}\frac{1}{m^3} \tag{23}$$

$$\tau_{tor} = \frac{3V}{b_0^2}\frac{t_{0,1}}{t_{net,0}}\left(\frac{1}{m} - \frac{1}{m^3}\right)k_b\gamma \qquad \text{with } k_b = \frac{2b_{max}b_0}{b_0^2 + b_{90}^2} \tag{24}$$

where

$$\gamma = \begin{cases} 1.5 & \text{for 3-layer CLT beams} \\ 0.2\dfrac{t_{0,2}}{t_{0,1}} + 1.1 & \text{for 5-layer CLT beams} \end{cases} \tag{25}$$

6.3 Comments on design proposals and concluding remarks

Both proposals are valid for 3- and 5-layer elements, with the restriction on element lay-up as $t_{0,2}/t_{0,1} = t_{0,2}/t_{0,3} \leq 2.0$ for 5-layer elements. The proposals are further limited in validity to element orientation such that the surface layers are oriented in the beam

length (x) direction. Further studies of CLT beam with inverted layer orientation and also studies of 7-layer elements should preferably be carried out.

A third proposal can be found from further simplification of design proposal 2, by using $\gamma = 1.5$ also for 5-layer CLT beams. This safe side assumption would render design equations no more complex, yet more accurate, than the equations found in the current draft version of the new Eurocode 5 (CEN/TC 250/SC5, 2018).

The proposals are based on assuming equal longitudinal lamination width b_0 for all m laminations in the beam height direction. Dimensions and placement of laminations with respect to the element edges are however in general not known in the actual design situation since the CLT beams in general are cut from larger elements, with no consideration of the location of the individual laminations. Following the recommendation in the draft version of the new Eurocode 5 (CEN/TC 250/SC5, 2018), in cases where the lamination width is not known, it should be assumed as $b_0 = b_{90} = 80$ mm.

The two proposals are solely based on comparison between analytical model predictions and FE-analyses, assuming the crossing area shear stress distributions and the failure criterion proposed by Flaig & Blass (2013) to be valid. Verification of the proposed models by comparison to experimental test results should be carried out.

7 Literature

Ansys Inc. 2018 (2017)

Bejtka I (2011): Cross (CLT) and diagonal (DLT) laminated timber as innovative material for beam elements. KIT, Karlsruhe, Germany.

CEN/TC 250/SC5 (2018): Working draft of design of cross laminated timber in a revised Eurocode 5-1-1, Version 2018-04-13, part of N892.

Danielsson H, Serrano E, Jeleč M, Rajčić V (2017a): In-plane loaded CLT beams – Tests and analysis of element lay-up. In: Proc. INTER, INTER/50-12-2, Kyoto, Japan.

Danielsson H, Jeleč M, Serrano E (2017b): Strength and stiffness of cross laminated timber at in-plane beam loading. Report TVSM-7164, Division of Structural Mechanics, Lund University, Sweden.

Danielsson H, Serrano E (2018): Cross laminated timber at in-plane beam loading – Prediction of shear stresses in crossing areas. Engineering Structures, https://doi.org/10.1016/j.engstruct.2018.03.018.

Flaig M (2013): Biegeträger aus Brettsperrholz bei Beanspruch in Plattebene. PhD thesis, KIT, Karlsruhe, Germany.

Flaig M, Blass HJ (2013): Shear strength and shear stiffness of CLT-beams loaded in plane. In: Proc. CIB-W18, CIB-W18/ 46-12-3, Vancouver, Canada.

Jeleč M, Rajčić V, Danielsson H, Serrano E (2016): Structural analysis of in-plane loaded CLT beam with holes: FE-analysis and parameter studies. In: Proc. INTER, INTER/49-12-2, Graz, Austria.